RESEARCH ARTICLE | DECEMBER 01 1998

Analysis and transition probabilities of the $A\,^1\Sigma^+ \rightarrow X\,^1\Sigma^+$ system of KH excited by the 4880 Å line of the argon ion laser

J. J. Camacho; J. M. L. Poyato; A. Pardo; D. Reyman

J. Chem. Phys. 109, 9372–9383 (1998)
https://doi.org/10.1063/1.477597

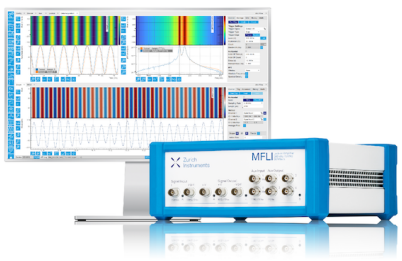

Analysis and transition probabilities of the $A\,^1\Sigma^+ \rightarrow X\,^1\Sigma^+$ system of KH excited by the 4880 Å line of the argon ion laser

J. J. Camacho, J. M. L. Poyato, A. Pardo, and D. Reyman
Departamento de Química-Física Aplicada, Facultad de Ciencias, Universidad Autónoma de Madrid, Cantoblanco, 28049-Madrid, Spain

(Received 9 June 1997; accepted 26 August 1998)

The fluorescence spectrum of KH induced by the 4880 Å line of an argon ion laser has been analyzed. This work extends previous observations on potassium hydride in visible region by using this excitation line. Along with the principal fluorescence series for the $A\,^1\Sigma^+ \rightarrow X\,^1\Sigma^+$ band system, corresponding to the excitation transition, $v'=7, J'=6 \leftarrow v''=0, J''=5$, we analyzed a very interesting satellite rotational and vibrational structure induced by collision. The radiative transition probabilities for the $A\,^1\Sigma^+ \rightarrow X\,^1\Sigma^+$ band system of KH have been calculated by using hybrid potential energy curves for the $X\,^1\Sigma^+$ and $A\,^1\Sigma^+$ states and transition dipole moment function from the radiative lifetimes of different vibrational levels ($v'=5-22$ in the $A\,^1\Sigma^+$ state) reported by Giroud and Nedelec. The transition probabilities and lifetimes are in good agreement with the corresponding observed measurements usually within the experimental uncertainty. Collision-induced rotational and vibrational energy transfer in the $A\,^1\Sigma^+$ state has been investigated. From the rotational and vibrational satellite structure of some bands, cross sections for rotational and vibrational energy transfer have been determined. © *1998 American Institute of Physics.* [S0021-9606(98)01145-3]

I. INTRODUCTION

The $A\,^1\Sigma^+ - X\,^1\Sigma^+$ band system of potassium hydride has been studied long ago through conventional spectroscopy[1–5] and laser spectroscopy.[6–13] A bibliography review of the most significant experimental measurements and theoretical calculations on KH is given by Stwalley *et al.*[14] More recently, Odashima *et al.*[15] have reported the first observation of pure rotational transitions in KH. Liu and Lin[16] have studied the rotational distribution of KH($v''=0-3$) produced in the reaction of K($5\,^2P$, $6\,^2P$ and $7\,^2P$) with H_2 by using a pump-probe technique. A recent study of the photoabsorption spectrum ($A\,^1\Sigma^+ \leftarrow X\,^1\Sigma^+$ band system) of potassium hydride[17] has revealed long v'-progressions with $v''=0$ and 1 up to a vibrational level with $v'=38$. Based on this analysis,[17] an extended RKR potential for the $A\,^1\Sigma^+$ state has been constructed by Rafi *et al.*[18] Because the highest observed vibrational level $v'=38$ has an energy about 1061 cm^{-1} above the atomic states to which the $A\,^1\Sigma^+$ dissociates, this electronic state must show a potential barrier.

On the other hand, the theoretical work on KH is concentrated mainly on describing potential energy curves, molecular properties and electric dipole moment functions for the lowest valence electronic states.[19–29] Although there is enough spectroscopic information available, theoretical investigations on radiative transition probabilities for the $A\,^1\Sigma^+ - X\,^1\Sigma^+$ system of this molecule are not reported, as the difficulty of electronic structure calculations increases rapidly with the number of electrons. Any accurate calculation of transition probabilities demands a knowledge on the variation of the electronic transition dipole moment versus internuclear distance. Particularly in diatomic systems such as the alkali hydrides, where the electronic transition moment of the $A-X$ transition displays a maximum (see for example Docken and Hinze,[30] Partridge and Langhoff[31] or Rerat *et al.*[32] for LiH, Sachs *et al.*[33] for NaH and Laskowski and Stallcop[34] for CsH) Franck-Condon factors and *R*-centroid calculations not yield quantitative results in studying intensity relations in a spectrum.

In this paper we have examined the fluorescence spectrum of the ^{39}KH vapor excited by the 4880 Å Ar^+ laser line. This exciting line induces only a single transition, $A\,^1\Sigma^+(v'=7, J'=6) \leftarrow X\,^1\Sigma^+(v''=0, J''=5)$.[6,11,13] Along with the corresponding fluorescence series of $R(5)$ and $P(7)$ doublets, we have analyzed in detail rotational and vibrational satellite lines induced by collision. The radiative transition probabilities for the $A\,^1\Sigma^+ - X\,^1\Sigma^+$ electronic band between $v' \leqslant 22$ vibrational levels of the excited state and all the vibrational levels of the ground state $v'' \leqslant 23$ have been calculated. Moreover for the principal fluorescence series $A\,^1\Sigma^+(v'=7, J'=6) \rightarrow X\,^1\Sigma^+(v''=0-23, J''=5,7)$ we have calculated the radiative transition probabilities and compared them with our experimental measurements. The radiative transition probabilities were calculated using hybrid potential energy curves for the $A\,^1\Sigma^+$ and $X\,^1\Sigma^+$ states and an electronic dipole moment function for the $A\,^1\Sigma^+ - X\,^1\Sigma^+$ transition from the radiative lifetimes of different vibrational levels ($v'=5-22$ in the $A\,^1\Sigma^+$ state) reported by Giroud and Nedelec.[9] Recently some studies, comparing radiative transition probabilities with experimental intensities using the laser-induced fluorescence technique have been reported by us.[35–37] We used photographic plates as our recording device with the intensity of fluorescence lines corrected by using a halogen lamp for calibration of the spectral

response of the spectrograph and plate. In order to obtain the best intensity measurements densitometries were recorded in the zone of the photoplate for which exposure remains within the linear zone of the photographic density range.

A comparison between theoretical and experimental values of radiative transition probability and lifetimes for the observed fluorescence series is made. Also, from the intensity ratio of satellite lines to parent lines, collision-induced rotational transition rates and average cross sections have been obtained for some bands of the spectrum.

II. EXPERIMENTAL DETAILS

An argon ion laser from Spectra Physics (Model 170) was tuned to 4880 Å, with an output of about 4.0 W at this wavelength. The potassium hydride vapor was produced by heating potassium with H_2 gas at an initial pressure of 10–20 Torr in a stainless steel heat pipe oven with cooled glass windows. The absorption of hydrogen by potassium begins at about 200 °C, and the metal absorbs about 125 times its own volume of hydrogen at temperatures in the range 300–400 °C. Potassium hydride can be also prepared by passing an electric arc between potassium metal rods in a stream of hydrogen. The heat pipe was normally set at $T \approx 430$ °C, which corresponds to a potassium vapor pressure of about 8 Torr while the vapor pressure of K_2 is about 0.1 Torr.[38] By using thermodynamic properties of gaseous potassium hydride reported by Mackay,[39] the partial pressure of KH at our working temperature is in the range 0.1–1 mTorr. No foreign gases were used in our experiments. The molecular fluorescence was observed in the opposite direction of the laser beam and, with the help of a lens, was imaged to the slit of the spectrometer. The detection system consisted of a high light-gathering 3 m modified Huet spectrograph. The nominal dispersion is 2.85 Å mm^{-1}. For the wavelength calibration we used the Ar^+ spectrum[40] (blue region) and a helium-neon laser multilined spectrum (red region). Another wavelength calibration of the KH fluorescence line positions is also available from the emission fluorescence of the Na_2 molecule induced under excitation by the argon laser line at 4880 Å. The total frequency range of the observations was in the visible region between 15100 and 21500 cm^{-1}. The line positions were measured on a manually operated comparator with an uncertainty of about ± 0.2 cm^{-1}. Each plate was measured three times. A least squares program fitting to an hyperbolic expression (Hartmann) was used to interpolate the fluorescence line positions from the calibration standards.

The relative intensity distribution of the resonance fluorescence spectra was obtained from the microdensitometry of the photographic plates. Later, the relative fluorescence intensities were corrected for the spectral response of spectrograph and plate. In order to make this calibration we used an Osram No. 6438; 6.6 A; 200 W halogen lamp.[41]

For each laser induced fluorescence spectrum, three exposures were necessary. The exposure time for each spectrum ranged from 30 min to 3 h. The microdensitometry was made by area integration in a rectangular region for which the exposure time was 30 min, in order to make sure that the work area remains within the linear part of the emulsion characteristic curve (graphical representation of the photographic densities against the logarithm of exposure). We estimate an uncertainty in the intensity measurement around 10%–20% for the most part of the lines. Only for some weak lines the uncertainty could be out of this interval.

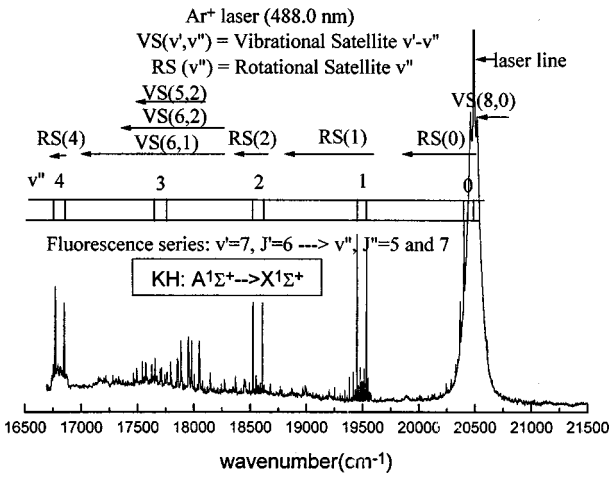

FIG. 1. Portion of the fluorescence spectrum of KH excited by the 4880 Å Ar^+ laser line. Along with the prominent $R(5)$ and $P(7)$ doublet fluorescence progression, the assignments of the rotational satellites [marked as RS(v'')] and the vibrational satellites [marked as VS(v',v'')] induced by collisions have been indicated.

III. SPECTROSCOPIC ASSIGNMENT

Figure 1 shows a portion (wavelength region, 4600–6500 Å) of the fluorescence lines in the spectrum of KH ($A-X$) excited by the 4880 Å argon ion laser line. This exciting line only populates one rovibronic level $v'_k=7$, $J'_k=6$ of the $A\,^1\Sigma^+$ state from the lower level $v''_0=0$, $J''_0=5$ in the $X\,^1\Sigma^+$ state. Thus we see the intense $R(5)$ and $P(7)$ doublet progression of vibrational bands starting at $v''=0$ and continuing up to $v''=6$ to the red of the exciting line. The excited KH molecules in the level populated by the laser suffer inelastic collisions with other atoms (K or H) or molecules (H_2, KH or K_2) being transferred into other adjacent vibrational-rotational levels $v'_k+\Delta v'$, $J'_k+\Delta J'$ of the same $A\,^1\Sigma^+$ state. The fluorescence from such adjacent levels produces satellite lines in the fluorescence spectrum. The fluorescence from the adjacent collision-induced rotational levels (v'_L, $J'_k+\Delta J'$) generates a rotational satellite RS(v'') structure around the v'' parent lines emitted from (v'_k, J'_k). Figure 1 shows such collision-induced rotational satellite lines RS(v'') around the parent $R(5)$ and $P(7)$ doublets for different v'' bands. These RS(v'') lines, as $J'_k=6$, are basically degraded to the red and their intensity is proportional to the intensity of the progression band $v'_k=7\rightarrow v''$. So, the most intense rotational satellite is RS($v''=1$) while RS($v''=3$) and RS($v''=6$) are not detected owing to the low intensity of the corresponding principal $R(5)$ and $P(7)$ doublets at $v''=3$ and $v''=6$. In Fig. 2 the assignment of the rotational transfer lines in the RS($v''=1$) band is indicated over each line. In Fig. 2 one recognizes rotational transitions with $\Delta J'$ up to $+16$ although, there are some unassigned lines, e.g., between $R(18)$ and $P(17)$ and between $P(18)$ and $R(20)$ which do not correspond to rotational satellites of the most

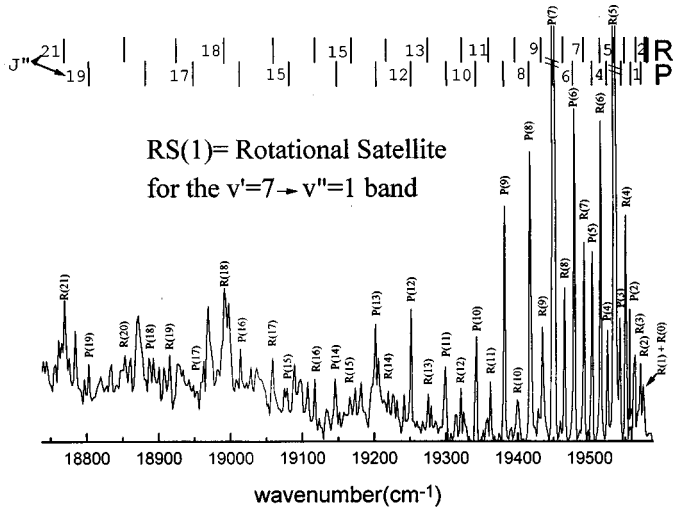

FIG. 2. Assignment of the rotational satellite lines for the most intense band with $v''=1$[RS(1)].

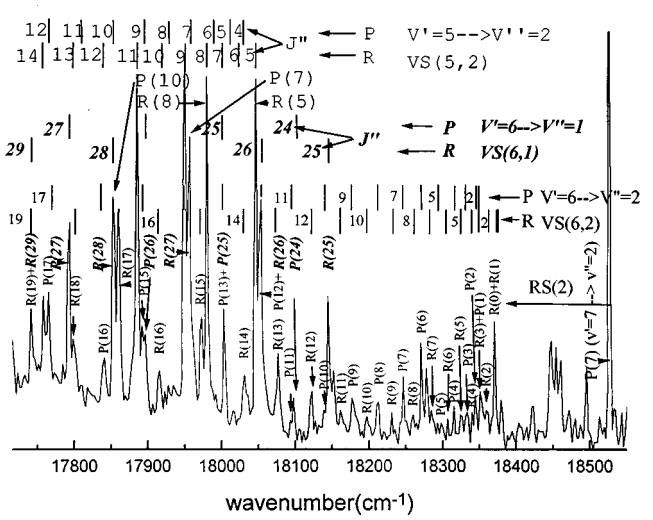

FIG. 3. Assignment of the vibrational satellite lines for the vibrational bands VS(6,2), VS(6,1) and VS(5,2) between 17800 and 18400 cm^{-1}.

intense $v'=7\rightarrow v''=1$ band. The large rotational spacing for KH permits a relatively easy identification of the satellite lines.

Other inelastic collision induced vibrational-rotational transitions $KH(v'_k, J'_k)\rightarrow KH(v'_k+\Delta v', J'_k+\Delta J')$ and the fluorescence from these last levels generates vibrational satellite bands $VS(v'_k+\Delta v', v'')$. Vibrational transfers corresponding to $\Delta v'=\pm 1$ and $\Delta v'=-2$ have been observed in the laser induced fluorescence spectrum. From Fig. 1 we see the vibrational satellites, VS(8,0), VS(6,1), VS(6,2) and VS(5,2), and their positions in the spectrum. To the anti-Stokes side of the exciting line (20486.65 cm^{-1}), the very weak vibrational satellite band VS(8,0) with lines corresponding to jumps with $\Delta J'=-2$ to $+6$ is observed [lines $P(5$ up to 13) and $R(3$ up to 11)]. Generally, the vibrational satellite lines are weaker than the rotational satellite lines (the cross sections are smaller). For example, Bergmann and Demtröder,[42] for various specified levels in $Na_2(B\,^1\Pi_u)$, found the total cross section for rotational energy transfer is the order of 100 $Å^2$ while the total vibrational cross section is about 10 $Å^2$ or less. However, as can be appreciated from Fig. 1, the intensity of the vibrational satellites VS(6,1), VS(6,2) and VS(5,2) (region 17200−18200 cm^{-1}) is even greater than the most intense rotational satellite RS($v''=1$). The fact that the weakness of the $R(5)$ and $P(7)$ doublet of the $v'=7\rightarrow v''=3$ band makes easy the observation of vibrational satellites with frequencies in this region. Other vibrational satellites were not detected perhaps owing to their low transition probabilities. Only the vibrational satellite VS(6,5) has a transition probability that would allow its observation in the $v'=7\rightarrow v''=6$ band region. However, its frequencies correspond to the beginning of K_2 absorption and its observation is quite difficult.

In Figs. 3 and 4 the assignment of the vibrational transfer lines is indicated over each line and with markers at the top of the figures corresponding to the calculated line positions. The vibrational satellite VS(6,2) appears with rotational lines from the band head $J'\approx 0$ up to lines with $J'\approx 26$. As the vibrational satellites VS(6,1), VS(6,2) and VS(5,2) appear in same region some lines are overlapped and higher resolving power is required. However, the optical resolution ≈ 0.2 cm^{-1} when we measured the spectral lines from a comparator is better than can be estimated from the figures of the spectrum. As KH has a light reduced mass, the rotational spacing is large if we compare with heavy molecules (for example, I_2 or Na_2) and it is possible to identify not only rotational doublets $P(J)$ and $R(J+2)$ but even lines of the same branch with J near to 0. The vibrational satellite VS(6,1) shows rotational lines from $J'\approx 24$ up to lines with $J'\approx 32$. The vibrational satellite VS(5,2) appears with rotational lines from $J'\approx 4$ up to lines with $J'\approx 21$.

In order to make the assignment of the spectrum we determined the frequency of the lines by using the molecular constants given in Stwalley *et al.*[14]

The intensities of vibrational satellite bands VS(v',v'') show a different behavior from each other. While VS(6,2) presents a regular profile with an intensity maximum around $J''=18$, the VS(6,1) shows lines with high J' values ($J'>20$). The VS(5,2) shows the most intense lines and appears

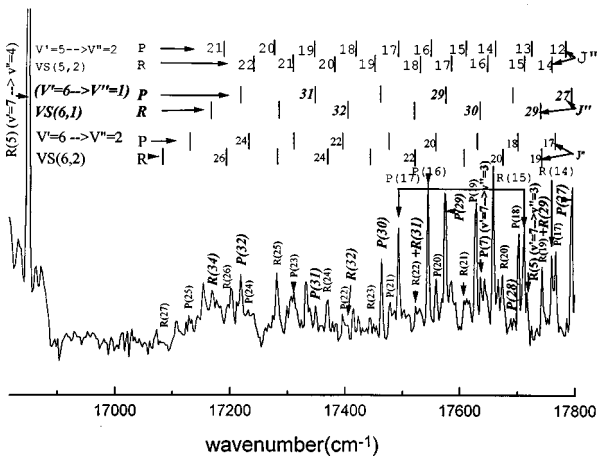

FIG. 4. Assignment of the vibrational satellite lines for the vibrational bands VS(6,2), VS(6,1) and VS(5,2) between 17000 and 17800 cm^{-1}.

TABLE I. RKR potential energy curve of the $X\,^1\Sigma^+$ state of KH including the Kaiser's correction. $Y''_{00}=0.67\text{cm}^{-1}$ and $r''_e=2.24032$ Å.

v	$G(v)+Y''_{00}(\text{cm}^{-1})$	B''_v (cm^{-1})	R_-(Å)	R_+(Å)
−0.5	0.67	3.41895	2.23342	2.24717
0	490.08	3.37384	2.07024	2.44599
1	1445.95	3.28951	1.96372	2.62286
2	2372.01	3.20664	1.89789	2.76008
3	3268.90	3.12423	1.84866	2.88250
4	4137.16	3.04299	1.80895	2.99714
5	4977.31	2.96304	1.77555	3.10722
6	5789.85	2.88383	1.74672	3.21460
7	6575.19	2.80477	1.72146	3.32058
8	7333.63	2.72560	1.69907	3.42612
9	8065.37	2.64643	1.67906	3.53195
10	8770.48	2.56747	1.66099	3.63869
11	9448.84	2.48863	1.64452	3.74698
12	10100.1	2.40924	1.62941	3.8575
13	10723.7	2.32802	1.61550	3.97136
14	11318.6	2.24325	1.60273	4.08973
15	11883.2	2.15302	1.59108	4.21442
16	12415.4	2.05526	1.58052	4.34793
17	12911.9	1.94742	1.57099	4.49398
18	13368.4	1.82544	1.56242	4.65841
19	13778.5	1.68246	1.55481	4.85122
20	14133.9	1.50761	1.54834	5.09071
21	14423.5	1.28669	1.54335	5.41421
22	14633.7	1.00700	1.53944	5.91484
23	14749.3	0.67042	1.53741	6.99334

from $J'=6$. This value coincides with the rotational quantum number of the laser pumped level. Some doublets of these vibrational satellites are indicated in Figs. 3 and 4. Generally the intensities of both the $R(J'')$ and the $P(J''+2)$ doublet lines originating from the same $J''+1$ rotational level agree with each other but some irregularities can be observed. In spite of these irregularities, the great number of measured lines in each vibrational satellite VS(v',v'') makes the assignments unambiguous. In order to avoid the problem with the irregular behavior of the intensities only the VS(6,2) band has been extensively studied.

IV. DETERMINATION OF TRANSITION PROBABILITIES

A. Construction of the potentials

Before proceeding to calculation of radiative transition probabilities, it is necessary to select adequate potential energy functions for both $A\,^1\Sigma^+$ and $X\,^1\Sigma^+$ electronic states and the $A-X$ dipole strength function. The potentials used in the present calculation were obtained basically from the information found in the literature for the KH, $A\,^1\Sigma^+$ and $X\,^1\Sigma^+$ electronic states. With the spectroscopic constants reported by Stwalley *et al.*[14] for the ground state of KH (where the rotational constants Y_{71}, Y_{81} and Y_{91} are corrected from the published numbers of Hussein *et al.*[13]) we determined the RKR points for the $X\,^1\Sigma^+$ state. Similarly, from the spectroscopic constants reported by Rafi *et al.*[18] for the $A\,^1\Sigma^+$ state of KH (obtained from the data of Bartky[5] and Rafi *et al.*[17]) we determined the RKR potential for the $A\,^1\Sigma^+$ state. Both RKR curves are given in Tables I and II. The RKR potential for the ground state is some different than the one reported by Hussein *et al.*[13] The slight differences in the usual RKR potentials are due to the method that is employed to handle the integrable singularity at the upper limit in the f and g integrals (Klein's equations)

$$f(v)=\frac{1}{2}(R_+-R_-)=\sqrt{\beta}\int_{v_0}^{v}\frac{dv'}{\sqrt{G(v)-G(v')}} \tag{1}$$

and

$$g(v)=\frac{1}{2}\left(\frac{1}{R_-}-\frac{1}{R_+}\right)=\frac{1}{\sqrt{\beta}}\int_{v_0}^{v}\frac{B'_v dv'}{\sqrt{G(v)-G(v')}}, \tag{2}$$

where R_+ and R_- are the classical turning points, $\beta=h/8\pi^2 c\mu$, v_0 is the value of the vibrational quantum number at the potential minimum $G(v_0)=0$, i.e., $v_0=-1/2-\Delta$ with $\Delta=(Y_{00}/Y_{10})[1+(Y_{00}Y_{20})/Y_{10}^2+\cdots]\approx Y_{00}/Y_{10}$ (Kaiser's correction[43]). In our treatment we removed the singularity through a simple change of variables such as it is reported by Telle and Telle.[44] Changing variables to avoid the singularity is effective; however, it requires a significant amount of computation time. We have tested that is equivalent removing the singularity through a subdivision of the integration interval

$$f(v)=\sqrt{\beta}\left(\int_{v_0}^{v-\delta}\frac{dv'}{\sqrt{G(v)-G(v')}}+\frac{2\sqrt{\delta}}{\sqrt{G'(v)}}\right) \tag{3}$$

and

$$g(v)=\frac{1}{\sqrt{\beta}}\left(\int_{v_0}^{v-\delta}\frac{B'_v dv'}{\sqrt{G(v)-G(v')}}+\frac{1}{\sqrt{G'(v)}}\int_{v-\delta}^{v}\frac{B'_v dv'}{\sqrt{v-v'}}\right), \tag{4}$$

where $G(v')$ has been expanded in a power series to first order about $v'=v$, δ is a number as small as possible (for KH, typically $\delta\approx 10^{-13}$) and the second integral in Eq. (4) can be evaluated analytically.

For the $X\,^1\Sigma^+$ state of KH, and exponential inner wall $U_{\text{in}}(R)=6.3434.10^6\exp[-3.94428\cdot R\ (\text{Å})]\ (\text{cm}^{-1})$ was constructed by fitting the *ab initio* points reported by Langhoff *et al.*[26] shifted to join smoothly the last inner RKR turning points. Also, as observed by Zemke and Stwalley,[45] the innermost RKR turning point for the last experimental vibrational level of the ground state calculated by us $R_-(v''=23)=1.52742$ Å is out of the line with the rest of the adjoining inner RKR turning points. Thus the new adjusted value is $R_-(v''=23)=1.53741$ Å and therefore the new corresponding maximum turning point is $R_+(v''=23)=6.99334$ Å, where the difference $R_+(v''=23)-R_-(v''=23)$ is preserved. The long-range region of the potential curve of the ground electronic state is represented by an inverse power expansion $-\Sigma_n C_n/R^n$ with $n=6,8$ and 10. The C_n coefficients are determined by least-squares onto the last outermost RKR turning points (generally ten points) and taking an asymptote at large internuclear distances corresponding to the dissociation limit energy. For the ground state potential the last available value for its dissociation energy was chosen [$D''_e=14772.7\ \text{cm}^{-1}$ (Ref. 45)]. The best fit parameters were $C_6=706783\ \text{cm}^{-1}\,\text{Å}^6$, $C_8=2.76692\cdot 10^6$

TABLE II. RKR potential energy curve of the $A\,^1\Sigma^+$ state of KH including the Kaiser's correction. $Y'_{00}=1.84$ cm^{-1} and $r'_e=3.76286$ Å. Also listed are the RKR classical turning points evaluated without Kaiser modification for comparison.

v	$G(v)+Y'_{00}$ (cm^{-1})	B''_v (cm^{-1})	R_-(Å)[a]	R_+(Å)[a]	R_-(Å)[b]	R_+(Å)[b]
−0.5	1.84	1.21908	3.70185	3.80288	-	-
0	114.94	1.24859	3.35147	4.13309	3.35410	4.12930
1	350.81	1.29889	3.07064	4.38732	3.07193	4.38495
2	598.24	1.33866	2.89053	4.55645	2.89142	4.55454
3	855.72	1.36914	2.75527	4.69380	2.75597	4.69215
4	1121.82	1.39147	2.64739	4.81489	2.64796	4.81342
5	1395.20	1.40669	2.55840	4.92666	2.55889	4.92531
6	1674.62	1.41571	2.48334	5.03284	2.48377	5.03159
7	1958.90	1.41941	2.41899	5.13565	2.41937	5.13448
8	2246.95	1.41854	2.36310	5.23652	2.36345	5.23542
9	2537.77	1.41380	2.31403	5.33642	2.31435	5.33538
10	2830.43	1.40577	2.27056	5.43602	2.27085	5.43503
11	3124.05	1.39500	2.23172	5.53582	2.23200	5.53487
12	3417.85	1.38195	2.19676	5.63619	2.19703	5.63528
13	3711.10	1.36702	2.16507	5.73742	2.16532	5.73654
14	4003.13	1.35056	2.13616	5.83974	2.13640	5.83889
15	4293.35	1.33286	2.10962	5.94334	2.10985	5.94253
16	4581.21	1.31414	2.08512	6.04840	2.08534	6.04760
17	4866.22	1.29462	2.06238	6.15504	2.06589	6.15426
18	5147.94	1.27445	2.04118	6.26340	2.04138	6.26264
19	5426.00	1.25373	2.02133	6.37359	2.02153	6.37285
20	5700.04	1.23257	2.00269	6.48573	2.00288	6.48501
21	5969.77	1.21100	1.98513	6.59993	1.98531	6.59923
22	6234.94	1.18909	1.96854	6.71628	1.96872	6.71559
23	6495.32	1.16683	1.95286	6.83489	1.95304	6.83422
24	6750.75	1.14425	1.93803	6.95586	1.93820	6.95520
25	7001.06	1.12133	1.92401	7.07929	1.92417	7.07863
26	7246.13	1.09807	1.91075	7.20526	1.91091	7.20462
27	7485.89	1.07446	1.89824	7.33389	1.89840	7.33326
28	7720.24	1.05049	1.88646	7.46526	1.88662	7.46438
29	7949.16	1.02619	1.87541	7.59947	1.87557	7.59886
30	8172.61	1.00155	1.86507	7.73662	1.86522	7.73601
31	8390.57	0.976631	1.85543	7.87679	1.85558	7.87619
32	8603.05	0.951486	1.84647	8.02009	1.84662	8.01950
33	8810.05	0.926207	1.83817	8.16661	1.83831	8.16603
34	9011.59	0.900913	1.83048	8.31646	1.83063	8.31588
35	9207.69	0.875763	1.82337	8.46972	1.82351	8.46915
36	9398.38	0.850955	1.81674	8.62652	1.81688	8.62595
37	9583.66	0.826733	1.81051	8.78696	1.81065	8.78639
38	9763.57	0.803391	1.80454	8.95117	1.80468	8.95062

[a]Evaluated with the Kaiser modification.
[b]Evaluated without the Kaiser modification.

cm^{-1} Å^8 and $C_{10}=-8.241\cdot10^9$ cm^{-1} Å^{10}. The values of C_n coefficients should not be compared with theoretical long range dispersion terms since all turning points distances are within 9 Å, the long range criterion distance of Leroy (see Ref. 47). The $X\,^1\Sigma^+$ potential curve reported here is not significantly different than the one reported by Zemke and Stwalley.[45]

The dissociation energy of the $A\,^1\Sigma^+$ excited state is calculated to be $D'_e=\nu_{\rm at}(\mathrm{K}\,^2P_{3/2,1/2}\rightarrow\mathrm{K}\,^2S_{1/2})+D''_e-T_e=8736\pm10$ cm^{-1}. The wave number of the atomic transition $\nu_{\rm at}(\mathrm{K}\,^2P_{3/2,1/2}\rightarrow\mathrm{K}\,^2S_{1/2})$ was calculated from the weighted average $[(2\nu_{3/2}+\nu_{1/2})/3]$ of the two atomic transitions, being $\nu_{3/2}(\mathrm{K}\,^2P_{3/2}\rightarrow\mathrm{K}\,^2S_{1/2})=13042.9$ and $\nu_{1/2}(\mathrm{K}\,^2P_{1/2}\rightarrow\mathrm{K}\,^2S_{1/2})=12985.16$ cm^{-1} (vacuum).[46] If we considered $\nu_{\rm at}=\nu_{1/2}$, we have $D'_e=8697\pm10$ cm^{-1}. On the basis of the value calculated for the dissociation energy of the $A\,^1\Sigma^+$ state, the highest observed vibrational level $v'=38$ has an energy of 1028 cm^{-1} (see Table II) above the states to which the such electronic excited state dissociates. This clearly shows that the upper electronic state has a barrier. In order to derive the long range part of the $A\,^1\Sigma^+$ potential including the potential barrier we fit the last ten maximum RKR turning points including an asymptote associates with the dissociation energy D'_e. We considered the following representation for the $A\,^1\Sigma^+$ potential barrier: $U(R)=C_0+C_6R^{-6}+C_8R^{-8}+C_{10}R^{-10}+A\cdot\exp(-B\cdot R)$. The least-squares adjusted parameters were $C_0=8736.7$ cm^{-1}, $C_6=-6.7916\cdot10^9$ cm^{-1} Å^6, $C_8=3.0074\cdot10^{12}$ cm^{-1} Å^8, $C_{10}=-7.3431\cdot10^{13}$ cm^{-1} Å^{10}, $A=-1.05253\cdot10^8$ cm^{-1} and $B=0.89$ Å^{-1} taking as zero point energy the minimum of the $A\,^1\Sigma^+$ potential curve. We estimated a barrier maximum of 1600 ± 500 cm^{-1}, relative to the $\mathrm{K}(4p)+\mathrm{H}(1s)$ atomic limit, located at 10.2 ± 0.5 Å. Naturally the

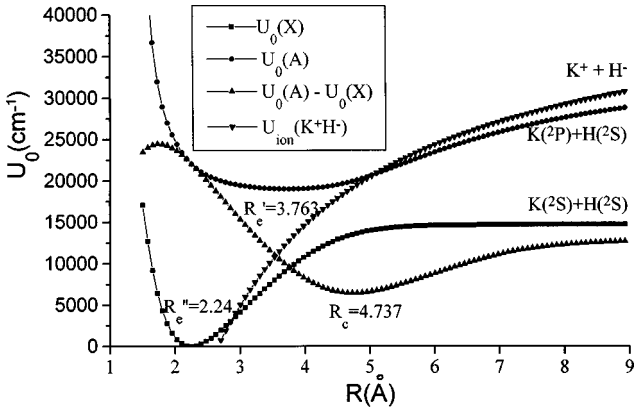

FIG. 5. Hybrid potential energy curves for the $X\,^1\Sigma^+$ and $A\,^1\Sigma^+$ states of KH. Also included are the ionic and the difference potential energy curves.

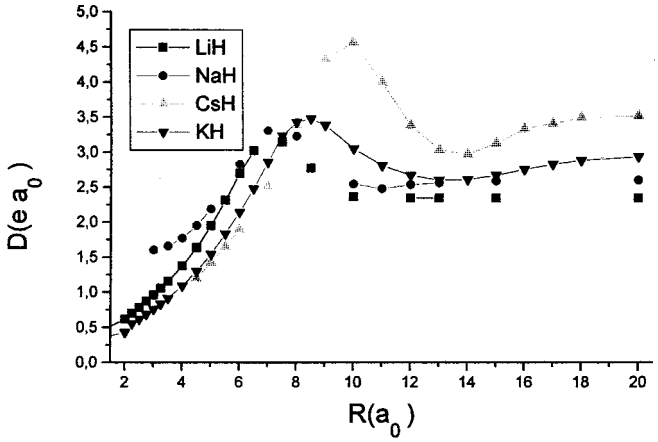

FIG. 6. Dipole strength function $D(R)$ (in atomic units) for the $A\,^1\Sigma^+ - X\,^1\Sigma^+$ transition of LiH, NaH, CsH and KH. See text for details.

estimated shape of the $A\,^1\Sigma^+$ potential barrier is only speculative and a detailed characterization requires experimental measurements (linewidth and energy) of the highest quasibound vibrational levels. The inner wall of the $A\,^1\Sigma^+$ potential curve consists of an exponential function of the form $U_{\text{in}}(R)=A\cdot\exp(-B\cdot R)+C$ based on a least squares fit of the last innermost RKR turning points. These parameters are as follows: $A=2.23064\cdot 10^8$ cm^{-1}, $B=5.9$ Å^{-1} and $C=4461.63$ cm^{-1}.

The RKR turning points for the $A\,^1\Sigma^+$ state obtained considering the Kaiser's correction (see above, where $Y'_{00}=1.845$ cm^{-1}) reported here (Table II) agree very well with the potential reported by Rafi *et al.*[18] For electronic states with high Y_{00} values, such as the $A\,^1\Sigma^+$ states of alkali hydrides, RKR calculations with or without Kaiser's correction should yield significant differences each other. In order to show this effect in the RKR calculation of the $A\,^1\Sigma^+$ state, Table II includes the turning points obtained using both methods. The two calculations deviate significantly from each other especially in the region around the bottom of the potential curve.

The RKR points were interpolated by a spline fit to obtain a smooth potential curvature. Thus the resulting hybrid potentials are then defined at all internuclear distances although the energy levels depend basically on the RKR region and only slightly on the exterior regions of extrapolation. The ground state $X\,^1\Sigma^+$ and the excited state $A\,^1\Sigma^+$ potential energy curves for KH obtained by the procedure above indicated are plotted in Fig. 5. This figure also shows the ionic potential curve adopted from the results by Yang and Stwalley[48] which includes a Born-Mayer repulsive term, the classical electrostatic term and a polarization term with a turning-off function.

B. Calculation of eigenvalues and eigenfunctions

Given the full hybrid potential without rotation $U_0(R)$ for the $X\,^1\Sigma^+$ and $A\,^1\Sigma^+$ states of KH we solve the radial Schrödinger equation (energy and potential in cm^{-1})

$$-\beta\frac{d^2\Psi_{v,J}}{dR^2}+\left[U_0(R)+\frac{\beta[J(J+1)-\Lambda^2]}{R^2}\right]\Psi_{v,J}(R)=E_{v,J}\cdot\Psi_{v,J}(R). \tag{5}$$

This equation was solved by finite difference method using a computer program developed in our laboratory. Derivatives of the unknown function $\Psi_{v,J}(R)$ in the differential equation are replaced by differences of the function at some chosen set of grid points. For linear homogeneous boundary value problems, defined by linear differential equations as Eq. (5), the finite difference method is very easy to use because leads to a matrix eigenvalue problem. For a second order differential equation the matrices are tridiagonal and an excellent numerical method exist to solve the resulting matrix eigenvalue problem.

We solved the radial wave equation for the fluorescence series $v'=7$, $J'=6\rightarrow v''=0-23$, $J''=5$ and 7 and for the vibrational levels $v'=0-22$ in the $A\,^1\Sigma^+$ state and $v''=0-23$ in the ground state. The calculated transition energies are, in general, within a few wave numbers of the corresponding experimental energies. For example, for the fluorescence series $v'=7$, $J'=6\rightarrow v''$, $J''=5$ and 7, the most striking deviation is for the last vibrational level $v''=23$ with $\Delta\nu$ (measured-calculated)$\simeq 1.5$ cm^{-1}.

C. The $A\,^1\Sigma^+ - X\,^1\Sigma^+$ transition dipole moment function

In order to calculate radiative transition probabilities it is necessary to know the functional representation for the $A\,^1\Sigma^+ \leftrightarrow X\,^1\Sigma^+$ transition dipole moment function $D(R)$. As far as we know, for KH there is not any *ab initio* quantum mechanical calculation of the $A\,^1\Sigma^+ \leftrightarrow X\,^1\Sigma^+$ band strength transition dipole moment function. Electronic transition moments as a function of internuclear separation for the $A\leftrightarrow X$ transition of other alkali hydrides have been reported for LiH,[30–32] NaH,[33] and CsH.[34] The $A\leftrightarrow X$ transition dipole function for these molecules is plotted in Fig. 6. The most noticeable feature in the internuclear distance R dependence of the $A\leftrightarrow X$ transition moments is the maximum in the vicinity of 7, 7 and 10 a_0, for LiH, NaH and CsH, respectively. This maximum appears approximately where both $A\,^1\Sigma^+$ and $X\,^1\Sigma^+$ states are 50% ionic-50% covalent. For KH we estimated this maximum lies around 8.5 a_0($\sim$4.5 Å). We

have constructed a dipole moment function for the $A\,^1\Sigma^+ \leftrightarrow X\,^1\Sigma^+$ electronic transition of KH assuming a similar functional form as other alkali hydrides. In a first failed attempt for constructing such function we have scaled the calculated points reported for LiH (Refs. 30–32) and NaH (Ref. 33) (the asymptotic limits are 2.35 and 2.59 a.u., respectively). Using these scaled $A \leftrightarrow X$ transition dipole moment functions we have computed the radiative lifetimes for the $A\,^1\Sigma^+$ state. For example, for the $v'=7$, $J'=6$, which is the only populated rovibrational level directly populated by the 4880 Å Ar^+ laser line, we calculated 28 and 26 ns, using the $D^{A-X}(R)$ scaled function of LiH and NaH, respectively. However, the experimental lifetime close to this level is $\tau_{v'=7,\,J'\simeq 9}=60$ ns.[9]

When the variation of dipole transition moment with internuclear distance is small, $D(R)$ can be displayed as a polynomial, which converges rapidly enough to take only into account the first two or three term in the sum, $D(R)=R_0+\alpha R+\beta R^2+\cdots$. In this case the connection between radiative lifetimes $\tau_{v'}$ and the dipole transition moment function $D(R)$ yields

$$\frac{1}{\tau_{v'}}=\frac{32\pi^3}{3\hbar}\sum_{v''}\ \nu^3_{v',v''}q_{v',v''}(R_0+\alpha R^c_{v',v''}+\beta R^{2c}_{v',v''}+\cdots)^2. \tag{6}$$

From all experimental lifetimes $\tau_{v'}$ of the upper vibrational levels reported by Giroud and Nedelec[9] and the necessary frequencies $\nu_{v',v''}$, Franck-Condon factors $q_{v',v''}$ and *R*-centroids $R^c_{v',v''}$ determined from the vibrational wave functions based on $A\,^1\Sigma^+$ and $X\,^1\Sigma^+$ potential curves, we obtained an electronic transition dipole moment function for the *r*-centroid region, $D(R)(e\cdot a_0)=-1.32+0.585R(a_0)$ with a $4.7<R(a_0)<8.5$ validity range. Values out of this range for $D(R)$ were determined by scaling the *ab initio* function for LiH and taking into account the asymptotic limit of KH. Considering the $K(4^2P_{3/2,1/2})-K(4^2S_{1/2})$ splitting and the corresponding oscillator strengths, f ($0.382\cdot 10^8$ and $0.387\cdot 10^8$ s^{-1}),[46] we find that the asymptotic limit of the $A \leftrightarrow X$ transition dipole moment function is 2.93 a.u. (7.45 Debyes). The $A \leftrightarrow X$ transition dipole moment function constructed for KH and used in our calculations is plotted in Fig. 6 and tabulated in Table III. From this function the calculated lifetime for the level excited by the laser line is $\tau_{v'=7,\,J'=6}=60.2$ ns. As transitions from vibrational levels of the $A\,^1\Sigma^+$ excited state with $v'>8$ include bound-free transitions (see below), in Eq. (6) these were considered by modified $\tau_{v'}$ experimental values. Spline fits were used to make continuous the electronic transition dipole moment function. The fitted transition dipole moment function $D(R)$ above indicated includes the ''anomalous'' radiative lifetime $\tau_{v'=22}=34$ ns (see Ref. 9). If this last vibrational level is not considered in the calculations, the transition dipole moment function changes strongly, $D(R)(e\cdot a_0)=-0.33+0.39R(a_0)$ with a $4.7<R(a_0)<8.5$ validity range.

TABLE III. Dipole strength function $D(R)$ in a.u. for the $A\,^1\Sigma^+-X\,^1\Sigma^+$ transition of KH.

$R(a_0)$	$D(R)(ea_0)$
1	0.333
2	0.493
2.25	0.556
2.5	0.619
3	0.762
3.25	0.836
3.5	0.914
4	1.09
4.5	1.295
5	1.543
5.5	1.833
6	2.139
6.5	2.476
7	2.857
7.5	3.238
8	3.429
8.5	3.476
9	3.381
10	3.048
11	2.809
12	2.667
13	2.6
14	2.60
15	2.667
16	2.750
17	2.825
18	2.875
20	2.930

D. Calculation of radiative transition probabilities

The interpretation of diatomic spectral line intensities has been well developed and thoroughly discussed in the literature.[49] In short, the theoretical intensity of a fluorescence emission line can be expressed as

$$I_{\text{thry}}=N_{v',J'}hc\nu A_{v',J'\rightarrow v'',J''}, \tag{7}$$

where $N_{v',J'}$ is the population in the excited level, ν is the fluorescence frequency for the corresponding transition $v',J'\rightarrow v'',J''$ and $A_{v',J'\rightarrow v'',J''}$ is the radiative transition probability of spontaneous emission. The population of the upper level is given by

$$N_{v',J'}\propto N_{v'',J''}B_{v',J'\leftarrow v'',J''}f(\Delta\nu) \tag{8}$$

being $N_{v'',J''}$ the population of the lower level, $B_{v',J'\leftarrow v'',J''}$ the absorption Einstein coefficient and $f(\Delta\nu)$ the relative overlap of the absorption line centered ν_0 with the Ar^+ laser line, a symmetric function of $\Delta\nu=\nu_{\text{laser}}-\nu_0$. At thermal equilibrium, the population of the lower rotational-vibrational levels follows a Boltzmann distribution

$$N_{v'',J''}=(2J''+1)\cdot e^{-[G''(v'')+F_{v''}(J'')]hc/kT}. \tag{9}$$

For KH at 700 K the maximum population is at $N_{v''=0,\,J''=8}\simeq 11$ assuming $N_{0,0}=1$. On the basis of this value it is clear that the excitation transitions must correspond basically from levels close to $v''=0$ and $J''=8$ because the number of KH molecules falls off very rapidly out of this range.

The Einstein $A_{v',J'\to v'',J''}$ coefficient of spontaneous emission for each v', $J'\to v''$, J'' bound-bound transition was calculated

$$A_{v',J'\to v'',J''} = \frac{64\pi^4\nu^3}{3h}\left|\int_0^\infty \Psi_{v',J'}(R)D(R)\Psi_{v'',J''}(R)dR\right|^2, \quad (10)$$

where $D(R)$ is the dipole strength function (transition moment) for the $A-X$ band system and $\Psi_{v',J'}(R)$ and $\Psi_{v'',J''}(R)$ are the radial wave functions for the upper $A\,^1\Sigma^+$ and lower $X\,^1\Sigma^+$ states. The total Einstein coefficient $A_{v',J'}$ arising from all bound-bound transitions in the $A\,^1\Sigma^+ - X\,^1\Sigma^+$ band system is given by the expression

$$A_{v',J'} = \frac{1}{2J'+1}\left[J'\sum_{v''=0}^{23} A_{v',J'\to v'',J'-1} + (J'+1)\sum_{v''=0}^{23} A_{v',J'\to v'',J'+1}\right]. \quad (11)$$

The calculated eigenfunctions $\Psi_{v,J}(R)$ and the $A-X$ electronic transition moment function reported in Table III were used for determining Einstein A coefficients [Eq. (10)]. In order to compare measured and theoretical relative intensities, we have considered the Einstein $A_{v',J'\to v'',J''}$ coefficient as the calculated intensity. These coefficients were initially obtained for the principal fluorescence series $v'=7$, $J'=6\to v''=0,\ldots,23$, $J''=5,7$. The experimental and theoretical intensities are normalized to the most intense fluorescence doublet lines $v'=7, J'=6\to v''=1, J''=5$ and 7. Frequencies, Franck-Condon factors $q_{v',J'\to v'',J''}=[\int_0^\infty \Psi_{v',J'}\times(R)\Psi_{v'',J''}(R)dR]^2$ and Einstein A coefficients of spontaneous emission for this fluorescence series are shown in Table IV and compared to experimental $R(5)$ and $P(7)$ lines in Fig. 7. The calculated radiative transition probabilities for the observed fluorescence lines are in good agreement with measured relative intensities.

The radiative lifetime $\tau_{v',J'}$ arising from all bound-bound transitions in the $A-X$ band system of KH were calculated as the reciprocal of the total Einstein $A_{v',J'}$ coefficients given in Eq. (11).

In a second stage, the radiative transition probabilities for the $A\,^1\Sigma^+ - X\,^1\Sigma^+$ electronic band between $v'\leqslant 22$ vibrational levels of the excited state and all the vibrational levels of the ground state $v''\leqslant 23$ have been calculated. Owing to the relative position of the potential energy curves of the $A\,^1\Sigma^+$ and $X\,^1\Sigma^+$ states of KH and the position of its corresponding vibrational levels, transition from vibrational levels of the A excited state with $v'\geqslant 8$ will be transitions to continuum. As can be seen in Table V, from the sum of the Franck-Condon factors $\Sigma_{v''}q_{v',v''}$ listed, already for $v'=10$ the R and P Franck-Condon factor sums for transitions to the ground state's bound levels account for approximately 80% of the total transition rate. The Franck-Condon factor sums decrease rapidly for higher vibrational levels and channels only the order of 30% into bound-bound transitions for the last vibrational level $v'=22$ calculated. Therefore for series with $\Sigma_{v''}^{23}q_{v',J'\to v'',J''}<1$ bound-free calculations are needed.

TABLE IV. Frequency, Franck-Condon factors and Einstein A coefficients of spontaneous emission for the fluorescence series $v'=7$, $J'=6\to v''=0-23$, $J''=5,7$.

v''	Line	Frequency (cm^{-1})	Q	$A^{A,v',J'}_{X,v'',J''}(s^{-1})$
0	$R(5)$	20487.45	0.5378E-1	0.17046E7
0	$P(7)$	20399.73	0.5220E-1	0.17304E7
1	$R(5)$	19534.11	0.9723E-1	0.30061E7
1	$P(7)$	19448.59	0.9255E-1	0.29840E7
2	$R(5)$	18610.53	0.4313E-1	0.12728E7
2	$P(7)$	18527.16	0.3736E-1	0.12047E7
3	$R(5)$	17716.11	0.5740E-3	0.19215E5
3	$P(7)$	17634.89	0.9537E-3	0.30937E5
4	$R(5)$	17850.30	0.4304E-1	0.12821E7
4	$P(7)$	16771.18	0.4257E-1	0.13128E7
5	$R(5)$	16012.54	0.4333E-1	0.12294E7
5	$P(7)$	15935.51	0.4188E-1	0.11749E7
6	$R(5)$	15202.38	0.9263E-3	0.23311E5
6	$P(7)$	15127.40	0.4889E-3	0.11797E5
7	$R(5)$	14419.41	0.2818E-1	0.73318E6
7	$P(7)$	14346.49	0.3010E-1	0.77357E6
8	$R(5)$	13663.34	0.4217E-1	0.10154E7
8	$P(7)$	13592.48	0.4093E-1	0.97296E6
9	$R(5)$	12933.97	0.1913E-2	0.39013E5
9	$P(7)$	12865.17	0.1162E-2	0.22634E5
10	$R(5)$	12231.24	0.2596E-1	0.56204E6
10	$P(7)$	12164.49	0.2816E-1	0.60099E6
11	$R(5)$	11555.25	0.3914E-1	0.76256E6
11	$P(7)$	11490.55	0.3753E-1	0.72059E6
12	$R(5)$	10906.34	0.3426E-3	0.42419E4
12	$P(7)$	10843.71	0.4792E-4	0.23736E3
13	$R(5)$	10285.19	0.3440E-1	0.59587E6
13	$P(7)$	10224.66	0.3666E-1	0.62541E6
14	$R(5)$	9692.85	0.2907E-1	0.45392E6
14	$P(7)$	9634.53	0.2632E-1	0.40518E6
15	$R(5)$	9130.01	0.4177E-2	0.59091E5
15	$P(7)$	9074.94	0.6132E-2	0.85562E5
16	$R(5)$	8601.67	0.4891E-1	0.63181E6
16	$P(7)$	8483.24	0.4879E-1	0.62145E6
17	$R(5)$	8108.38	0.2746E-2	0.35149E5
17	$P(7)$	8057.76	0.1245E-2	0.16515E5
18	$R(5)$	7655.63	0.4353E-1	0.44683E6
18	$P(7)$	7608.17	0.4589E-1	0.46571E6
19	$R(5)$	7249.80	0.1113E-2	0.19500E5
19	$P(7)$	7206.06	0.1771E-4	0.29587E4
20	$R(5)$	6899.65	0.2251E+0	0.16134E7
20	$P(7)$	6860.46	0.2461E+0	0.17408E7
21	$R(5)$	6616.65	0.1288E+0	0.80732E6
21	$P(7)$	6583.20	0.1014E+0	0.62050E6
22	$R(5)$	6414.81	0.3857E-1	0.24922E6
22	$P(7)$	6388.63	0.4169E-1	0.26178E6
23	$R(5)$	6309.28	0.4550E-2	0.32325E5
23	$P(7)$	6291.85	0.4169E-1	0.25131E6

The total Einstein A coefficient for a transition from a specific rovibrational level (v',J') of the excited state has been obtained from the expression

$$A^{\text{total}}_{v',J'} = A^{\text{bound-bound}}_{v',J'} + A^{\text{bound-free}}_{v',J'}. \quad (12)$$

The Einstein A coefficient to continuum states with wave number k'', being $k''^2\hbar^2/2\mu$ the asymptotic kinetic energy, can be calculated as

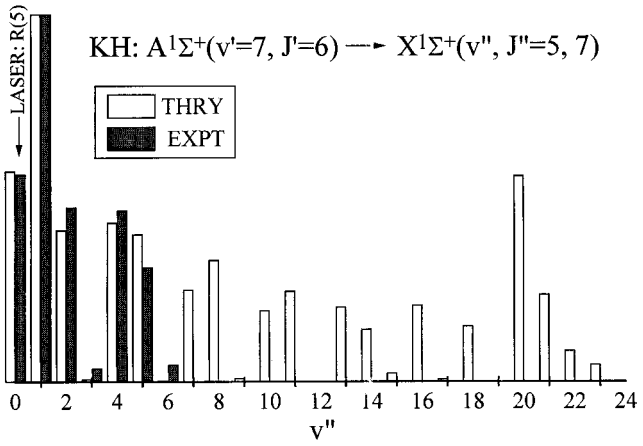

FIG. 7. Relative intensities (experiment, solid bars and theoretical, hollow bars) for the fluorescence series of the R and P lines $v'=7$, $J'=6\rightarrow v''$, $J''=5$ and 7 (average) in the $A\,^1\Sigma^+\rightarrow X\,^1\Sigma^+$ spectrum of KH excited by an Ar^+ (4880 Å) laser.

$$A^{\text{bound-free}}_{v',J'\rightarrow k'',J''} = \frac{64\pi^4\nu^3}{3h}\left|\int_0^\infty \Psi_{v',J'}(R)D(R)\Psi_{k'',J''}(R)dR\right|^2. \qquad (13)$$

The continuum wave functions can be calculated using energy normalization for the free wave, i.e., $k''^2=2\mu E/\hbar^2$. This can be achieved by normalizing the amplitude of the wave function in the range of internuclear distances and then multiplying by the energy. Generally, only the continuum wave functions close to the dissociation limit of the $X\,^1\Sigma^+$ state will contribute significantly to the transition probability since for higher kinetic energies the wave functions oscillate rapidly and overlap contributions cancel out. We have obtained continuum wave functions $\Psi_{k'',J''=5\text{ and }7}(R)$ up to a kinetic energy about of 3000 cm^{-1} above the atomic limit $K(4s)+H(1s)$, with a spacing of 2 cm^{-1} for energies close to dissociation limit of the ground state and increasing to larger separations up to 20 cm^{-1} for higher energies. Values for even higher kinetic energies were investigated but were found to result in only insignificant contributions. However, it is not possible to know the kinetic energy of continuum levels above the dissociation limit of the X state that really contribute continuous bound-free emission because for the $A-X$ system of KH there is no such experimental information. Therefore, the corresponding energy of continuum wave functions $\Psi_{k'',J''}(R)$ is chosen somewhat arbitrary. Moreover, different extrapolations of the inner wall of the $X\,^1\Sigma^+$ potential (this region of the potential is constructed beyond the experimental data) cause important variations in the position of the nodes of continuum wave functions $\Psi_{k'',J''}(R)$ and therefore the calculation of the $A^{\text{bound}-\text{free}}_{v',J'\rightarrow k'',J''}$ coefficients may be fairly imprecise. Owing to these problems, for the calculation of these one coefficients we have considered the experimental lifetimes reported by Giroud and Nedelec.[9]

It is useful to discuss the bound-free transitions in terms of the Mulliken difference potential,[50]

$$\begin{aligned}\text{MDP}(R) &= \text{KE}_{v',J'}(R)+U^X_{J''}(R)\\ &= E_{v',J'}(R)-U^A_{J'}(R)+U^X_{J''}(R),\end{aligned} \qquad (14)$$

where $\text{KE}_{v',J'}(R)$ is the classical nuclear kinetic energy at

TABLE V. Franck-Condon factors, bound-bound (bb), bound-free (bf) and total Einstein $A_{v',J'}$ coefficients and radiative lifetime of the various vibrational levels v' of the $A\,^1\Sigma^+$ state of KH. All Einstein A coefficients are in units of 10^6 s^{-1}. The lifetimes (interpolated from Ref. 9) are in ns.

	$P(7)$ lines			$R(5)$ lines				
v'	$\Sigma^{23}_{v''}q_{v',J'-v'',J''}$	$A^{b\text{-}b}_{v',J'}$	$A^{b\text{-}f}_{v',J'}$	$\Sigma^{23}_{v''}q_{v',J'-v'',J''}$	$A^{b\text{-}b}_{v',J'}$	$A^{b\text{-}f}_{v',J'}$	A_{tot}	$\tau^{\text{exp}}_{v',J'\sim 8-9}$
0	1.000	8.231	0.000	1.000	7.125	0.000	15.356	
1	1.000	8.631	0.000	1.000	7.471	0.000	16.102	
2	1.000	8.921	0.000	1.000	7.722	0.000	16.643	
3	1.000	9.069	0.000	1.000	7.850	0.000	16.919	
4	1.000	9.108	0.000	1.000	7.884	0.000	16.993	
5	1.000	9.064	0.000	1.000	7.845	0.000	16.908	64
6	1.000	8.994	0.000	1.000	7.772	0.000	16.767	61.6
7	1.000	8.959	0.000	1.000	7.661	0.000	16.691	60
8	0.923	8.576	0.513	0.903	7.357	0.502	16.949	59
9	0.781	7.932	1.073	0.820	6.991	1.127	17.123	58.4
10	0.821	7.994	1.290	0.771	6.745	1.212	17.241	58
11	0.713	7.426	2.114	0.616	6.086	1.826	17.452	57.3
12	0.597	6.812	2.646	0.552	5.765	2.446	17.668	56.6
13	0.658	7.071	2.731	0.560	5.730	2.325	17.857	56
14	0.691	7.240	2.931	0.538	5.566	2.282	18.018	55.5
15	0.477	5.943	3.577	0.469	5.145	3.517	18.182	55
16	0.450	5.738	3.745	0.460	5.036	3.827	18.349	54.5
17	0.508	6.102	3.937	0.455	4.955	3.526	18.519	54
18	0.375	5.109	3.940	0.452	4.893	4.749	18.692	53.5
19	0.343	4.814	4.131	0.431	4.733	5.190	18.868	53
20	0.378	5.058	5.145	0.397	4.474	5.403	20.080	49.8
21	0.292	4.281	5.910	0.404	4.515	8.177	22.883	43.7
22	0.285	4.173	9.446	0.352	4.126	11.67	29.412	34

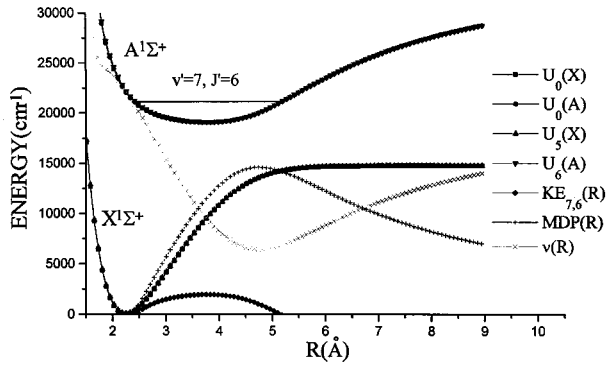

FIG. 8. Hybrid potential energy curves and effective potential with $J''=5$ and $J'=6$ for the $X\,^1\Sigma^+$ and $A\,^1\Sigma^+$ states of KH. Also included are the classical nuclear kinetic $KE_{v'=7,\,J'=6}(R)$ energy curve, Mulliken difference potential MDP(R) and the corresponding frequency of emission $\nu(R)$. The maximum of the MDP occurs at an energy of 14613 cm^{-1} at an internuclear distance of 4.725 Å. The maximum of the classical kinetic energy for the $v'=7$, $J'=6$ level occurs at an energy of 1967 cm^{-1} at an internuclear distance of 3.763 Å.

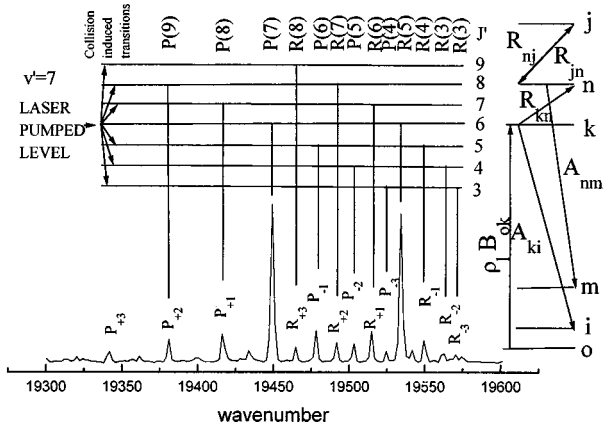

FIG. 9. Rotational transitions for the $v'_k=7$, $J'_k=6$ level in the $A\,^1\Sigma^+$ state of KH. Some lines of resulting spectrum are shown at the bottom. Also it is indicated a diagram illustrating rate equations.

internuclear distance R and $U_J(R)$ is the effective potential. The Mulliken difference potential function corresponds to the application of the Franck-Condon principle that the nuclear kinetic energy is conserved during an electronic transition. The corresponding frequency of emission at R is

$$\nu(R)=E_{v',J'}-\mathrm{MDP}(R)=U^A_{J'}(R)-U^X_{J''}(R). \tag{15}$$

In Fig. 8 are shown the potential energy curves without rotation $U_0(R)$, the effective potentials $U_J(R)$, the Mulliken difference potential MDP(R), the classical nuclear kinetic energy $KE_{v'=7,\,J'=6}(R)$ and the emission frequency $\nu(R)$ for the A and X electronic states of KH. From the shape of the MDP(R) function (the most simple cases are monotonic, single extremum and double extrema) it is possible to know approximately the possible structure of the bound-free emission.[50] In Fig. 8 MDP(R) corresponds to a single extremum case. Thus there will be two internuclear distances for most classical emission frequencies up to a limit (extreme or ''satellite'' frequency) and none past that frequency. This will impose an additional modulation on the rapid ''wave function'' oscillations which always occur. Also there will be a fairly sharp cutoff beyond the satellite position, which itself will be relatively intense as $d\mathrm{MDP}/dR$ goes to zero ($R\sim 4.7$ Å).

V. COLLISION-INDUCED TRANSITION RATES

Significant progress has been made in the study of state specific collision-induced rotational and vibrational energy transfer in diatomic molecules. Some examples of works on rotational-vibrational energy transfer can be found in the following references: 51, 42, and 52–57.

As mentioned earlier, the KH molecules (N_k) in the vibrational-rotational level $v'_k=7$, $J'_k=6$ of the $A\,^1\Sigma^+$ state selectively populated by the laser line suffer inelastic collisions, being transferred into other vibrational-rotational levels v'_n, J'_n of the same $A\,^1\Sigma^+$ state. An illustration of different processes that can occur is shown in Fig. 9. Also the collision-induced rotational satellite lines are shown at the bottom of the figure for the $v'=7\rightarrow v''=1$ vibrational band. The rate for the depopulation of the vibrational-rotational level k is the sum of spontaneous rate $\Sigma_i \overset{A_{ki}}{A_{ki}} N_k$ into lower levels i, i.e., $\mathrm{KH}(v'_k=7,\ J'_k=6)\rightarrow \mathrm{KH}(v''_i,\ J''_i)$ (parent lines), and the relaxation rate $\Sigma_n R_{kn} N_k$ produced by collision-induced radiationless transitions into other levels of the excited state, i.e., $\mathrm{KH}(v'_k=7, J'_k=6) \overset{R_{kj}}{\rightsquigarrow} \mathrm{KH}(v'_n,\ J'_n)$

$$\frac{dN_k}{dt}=-\left(\sum_i A_{ki}+\sum_n R_{kn}\right)N_k. \tag{16}$$

The fluorescence from the n levels $\mathrm{KH}(v'_n,\ J'_n) \overset{A_{nm}}{\rightarrow} \mathrm{KH}(v''_m,\ J''_m)$ populated by collision-induced transitions produces satellite lines around the parent lines from the emission from the pumped k level. Moreover the collisionally populated level n can be also populated and depopulated by two successive collision-induced radiationless transitions $\mathrm{KH}(v'_n, J'_n) \overset{R_{nj}}{\underset{R_{jn}}{\rightsquigarrow}} \mathrm{KH}(v'_j,\ J'_j)$. Under stationary conditions, the rate equation for the population N_n is given by

$$\frac{dN_n}{dt}=0=N_k R_{kn}+\sum_j N_j R_{jn}-\left(\sum_m A_{nm}+\sum_j R_{nj}\right)N_n. \tag{17}$$

At lower pressures, if the terms R_{jn} and R_{nj} which describe two successive collision-induced transitions may be neglected, the stationary population density N_n is given by

$$N_n=N_k\frac{R_{kn}}{\Sigma_m A_{nm}}. \tag{18}$$

The intensity ratio of satellite lines to parent lines is given by

$$\frac{I^{\mathrm{satellite}}_{nm}(v'_n,J'_n\rightarrow v''_m,J''_m)}{I^{\mathrm{parent}}_{ki}(v'_k,J'_k\rightarrow v''_i,J''_i)}=\frac{N_n A_{nm} h\nu_{nm}}{N_k A_{ki} h\nu_{ki}}. \tag{19}$$

Inserting Eq. (18) into Eq. (19), with $\Sigma_m A_{nm}=1/\tau_n$, yield the collision-induced transition rate R_{kn}

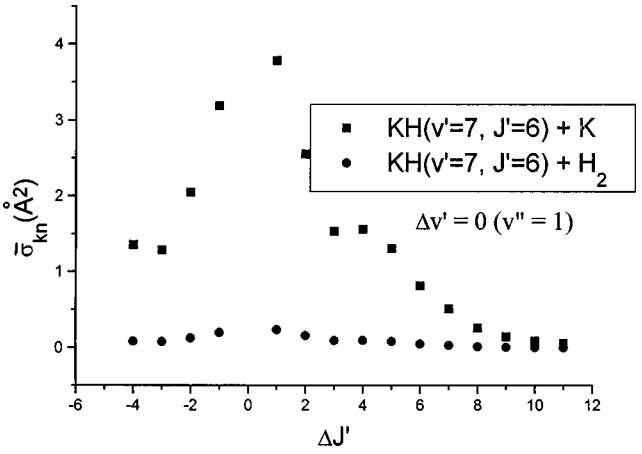

FIG. 10. Cross sections for collision-induced rotational transitions in the KH($v'=7, J'=6$) (from the $v'=7\rightarrow v''=1$ vibrational band) as a function of quantum jump $\Delta J'$ for collisions KH+K and KH+H_2.

$$R_{kn}=\frac{I_{nm}^{\text{satellite}}A_{ki}\nu_{ki}}{I_{ki}^{\text{parent}}A_{nm}\nu_{nm}\tau_n}. \tag{20}$$

At thermal equilibrium, by assuming that collisions between excited molecules can be neglected ($N_{\text{KH}^*(v'_k=7,\,J'_k=6)}\ll N_{\text{B(collision-partner)}}$) and if the cross section is not critically dependent on relative velocity of collision partners, the average cross section $\overline{\sigma_{kn}}$ can approximate to the collision-induced transition rate R_{kn} by

$$\overline{\sigma}_{kn}=R_{kn}\sqrt{\frac{kT\pi\mu}{8}}\,\frac{1}{P}, \tag{21}$$

where k is the Bolzmann's constant and T is the temperature. In Eq. (21) P is the pressure of the collision partner and μ is the reduced mass of the system KH−B(collision−partner) ($1/\mu=1/M_{\text{KH}}+1/M_{\text{B}}$).

A. Rotational transfers

As described earlier (see Fig. 1) a satellite rotational and vibrational structure has been assigned. For our experimental conditions, $T=700$ K (vapor pressure of KH around 8 Torr) and initial H_2 pressures between 10 and 20 Torr, the primary collision partners of KH($v'=7, J'=6$) excited molecules are potassium atoms and hydrogen molecules. By using Eqs. (20) and (21) we have calculated the average cross section assuming both collision partners. In Fig. 10 the absolute values of rotational cross sections are shown for the most intense $v'=7\rightarrow v''=1$ vibrational band for quantum jumps from $\Delta J'=-6$ up to $\Delta J'=+11$ for collisions KH($v'=7, J'=6$)+K and KH($v'=7, J'=6$)+H_2. The cross sections for $\Delta J'=\pm 1$ transitions are of the order of 4 Å^2 and decrease with increasing $|\Delta J|$. The uncertainties in the cross sections, including the measurement of the area of lines and errors in measuring pressure and temperatures are less than 20% for lower $|\Delta J|$ transitions and increase to about 30% for upper $|\Delta J|$ transitions. The cross sections for collisional-induced rotational transitions depend on the rotational energy transfer $\Delta E_r=E(v'_k=7, J'_k=6)-E(v'_k, J'_k+\Delta J')$ and decrease with increasing energy. The relative decrease of the cross section with increasing $|\Delta J|$ indicates that the decrease is due to increment of angular momentum to be exchanged.

For the $v'=7\rightarrow v''=0$ vibrational band the measurements of collision induced satellite rotational lines could be extended for quantum jumps from $\Delta J'=-3$ up to $\Delta J'=+8$. For the other intense $v'=7\rightarrow v''=2$ vibrational band the measurements of collision induced satellite rotational lines could be extended for quantum jumps from $\Delta J'=-5$ up to $\Delta J'=+7$. In this way, for our experimental conditions, the dominant collision partner of excited KH molecules in the level pumped by the 4880 Å laser line could be potassium atoms. This fact agrees with experimental results of Hussein *et al.*[13] In their experimental conditions ($T=763$ K, with a pressure maintained at 5.3 Torr using Ar as buffer gas and trace amounts of H_2), they observed rotational satellites around the two $R(5)$ and $P(7)$ parent lines for the most intense vibrational bands. We have estimated the cross sections for their rotational satellite transitions induced by the collision of KH+Ar in the $v'=7-v''=0$ vibrational band to be of the order of 2.4 Å^2 for $\Delta J'=\pm 1$ transitions, decreasing to 0.7, 0.4, 0.2 and 0.1 Å^2 for $\Delta J'=\pm 2$, ± 3, ± 4 and ± 5, respectively.

B. Vibrational transfers

As mentioned above collision induced vibrational transitions for the (v',v'') bands (8,0), (6,1), (6,2) and (5,2) were observed (see Figs. 3 and 4). Collision-induced vibrational transfers in KH produced in a discharge have been reported by Giroud and Nedelec.[9] In their experiments, the hydrogen pressure varied from 5×10^{-2} to 1 Torr and the temperature was fixed around 600 K. In the discharge they observed rotational and vibrational transfers with $\Delta v'=\pm 1$ and ± 2 and after the discharge the vibrational transfers disappeared whereas the rotational transfers remained. Therefore, it is possible to attribute the vibrational transfer to collision between excited KH and electrons and the rotational transfer to collision with H_2 or potassium. In such experiments, as the energy of the electrons was much greater than the energy exchanged in the collision, a symmetric decrease as $|\Delta v'|$ increases was observed owing to the variation in the transition probability. However, for our experimental conditions, the intensity of the vibrational satellite with $\Delta v'=+1$ (only some rotational lines of the satellite $v'=8-v''=0$ were detected) is lowest than vibrational transfer with $\Delta v'=-1$ and $\Delta v'=-2$ suggesting that this behavior is due to the variation of the energy transferred during the collision, the transition probabilities being less important.

Vibrational transitions were studied in a similar way to rotational transitions. Unfortunately many lines of collision-induced vibrational satellite lines VS(6,1) and VS(5,2) are overlapped and they were not considered in the present study. As the rotational structure of the $v'=6-v''=2$ band is very extended with R and P doublets from $J'=0$ to $J'=27$ we have studied especially this vibrational satellite. First we determined the intensity distribution for different rotational quantum numbers J' (band shape). The band shape is similar to the calculated cross section shown in Fig. 11. Looking at this last figure, one can easily recognize a maximum towards $J'=18$. Taking into account the rovibrational level $v'=6$, $J'=15$ has approximately the same energy as the level directly populated by the laser, the maxi-

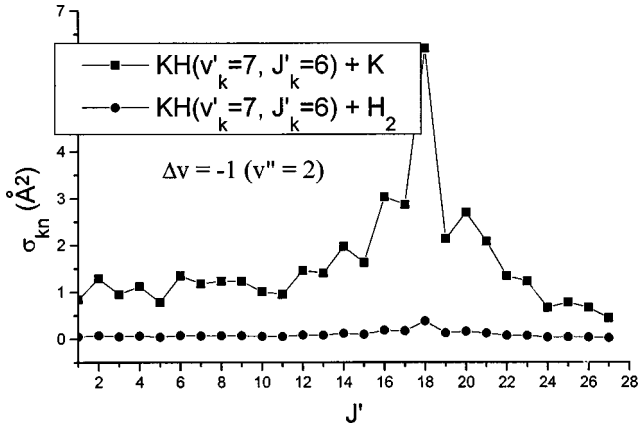

FIG. 11. Cross sections for collision-induced vibrational rotational transitions in the KH($v'=7, J'=6$) (from the $v'=6 \rightarrow v''=2$ vibrational band) as a function of quantum jump $\Delta J'$ for collisions KH+K and KH+H_2.

mum efficiency in the vibrational-rotational energy transfer could be around $J'=15$; in this case $J'=18$. Evidently molecules with small reduced mass such as KH (for which the rotational spacing is high) a decrease of the vibrational energy is accompanied by a net increase of the angular momentum and rotational energy of molecule, while molecules with larger reduced mass retain more easily the angular momentum and rotational energy in the collision (see Bergmann and Demtröder[42] for Na_2).

The cross sections for vibrational transitions were obtained by using Eqs. (19) and (20) and by considering as a collision partner of excited KH both H_2 and K atoms. Similar to the case of cross sections for collision-induced rotational transitions for our experimental conditions, the most probable collision partners of KH excited molecules are K atoms instead of H_2 molecules.

At present we are measuring effective lifetimes of different levels in the $A\,^1\Sigma^+$ excited state of KH, by varying the H_2 pressure and temperature (vapor pressure of K), in order to obtain Stern-Vollmer plots that unambiguously determine the collision partner in our experiments.

ACKNOWLEDGMENTS

We gratefully acknowledge the support received from the DGICYT (Spain) (Project No. PB96-0046) for this research.

[1] G. M. Almy and C. D. Hause, Phys. Rev. **42**, 242 (1932).
[2] T. Hori, Mem. Ryojun College Eng. **6**, 1 (1933); **6**, 115 (1933).
[3] S. Imanishi, Sci. Pap. Inst. Phys. Chem. Res. (Jpn.) **39**, 45 (1941).
[4] G. M. Almy and C. M. Beiler, Phys. Rev. **61**, 242 (1942).
[5] I. R. Bartky, J. Mol. Spectrosc. **20**, 299 (1966); **21**, 1 (1966); **21**, 25 (1966).
[6] J. A. Cruse and R. N. Zare, J. Chem. Phys. **60**, 1182 (1974).
[7] S. C. Yang, Y. K. Hsieh, K. K. Verma, and W. C. Stwalley, J. Mol. Spectrosc. **83**, 304 (1980).
[8] M. Giroud and O. Nedelec, J. Chem. Phys. **73**, 4151 (1980).
[9] M. Giroud and O. Nedelec, J. Chem. Phys. **77**, 3998 (1982).
[10] M. Giroud and O. Nedelec, Chem. Phys. **93**, 127 (1983).
[11] A. Pardo, J. M. L. Poyato, M. S. Guijarro, and J. I. F. Alonso, J. Mol. Spectrosc. **97**, 248 (1983).
[12] N. N. Haese, D. L. Liu, and R. S. Altman, J. Chem. Phys. **81**, 3766 (1984).
[13] K. Hussein, C. Effantin, J. d'Incan, J. Verges, and R. F. Barrow, Chem. Phys. Lett. **124**, 105 (1986).
[14] W. C. Stwalley, W. T. Zemke, and S. C. Yang, J. Phys. Chem. Ref. Data **20**, 153 (1991).
[15] H. Odashima, B. Wang, F. Matsushima, S. Tsunekawa, and K. Takagi, J. Mol. Spectrosc. **171**, 513 (1995).
[16] D. K. Liu and K. C. Lin, J. Chem. Phys. **105**, 9121 (1996).
[17] M. Rafi, N. Ali, K. Ahmad, I. A. Khan, M. A. Baig, and Z. Iqbal, J. Phys. B **26**, L129 (1993).
[18] M. Rafi, R. Al-Tuwirqui, and Fayyazuddin, J. Phys. B **29**, L533 (1996).
[19] R. Grice and D. R. Herschbach, Mol. Phys. **27**, 159 (1974).
[20] S. A. Adelman and D. R. Herschbach, Mol. Phys. **33**, 793 (1977).
[21] R. W. Numrich and D. G. Truhlar, J. Chem. Phys. **79**, 2745 (1975); **82**, 168 (1978).
[22] C. F. Melius, R. W. Numrich, and D. G. Truhlar, J. Chem. Phys. **83**, 1221 (1979).
[23] B. C. Garret, M. J. Redmon, and C. F. Melius, J. Chem. Phys. **74**, 412 (1981).
[24] W. J. Stevens, A. M. Karo, and J. R. Hiskes, J. Chem. Phys. **74**, 3989 (1981).
[25] G. H. Jeung, J. P. Dauley, and J. P. Malrieu, J. Phys. B **16**, 699 (1983).
[26] S. R. Langhoff, C. W. Bauschlicher, Jr., and H. Patridge, J. Chem. Phys. **85**, 5158 (1986).
[27] B. Bussery, M. Aubert-Frécon, and M. Saute, Chem. Phys. **109**, 39 (1986).
[28] P. Fuentealba, O. Reyes, H. Stoll, and H. Preuss, Chem. Phys. Lett. **87**, 5338 (1987).
[29] A. Ross, B. Bussery, G. H. Jeung, M. C. Bacchus-Montabonel, and M. Aubert-Frécon, J. Chem. Phys. **84**, 745 (1987).
[30] K. K. Docken and J. Hinze, J. Chem. Phys. **57**, 4936 (1972).
[31] H. Partridge and S. Langhoff, J. Chem. Phys. **74**, 2361 (1981).
[32] M. Rerat, C. Pouchan, M. Tedjeddine, J. P. Flament, H. P. Gervais, and G. Berthier, Phys. Rev. A **43**, 5832 (1991).
[33] E. S. Sachs, J. Hinze, and N. H. Sabelli, J. Chem. Phys. **62**, 3384 (1975).
[34] B. Laskowski and J. R. Stallcop, J. Chem. Phys. **74**, 4883 (1981).
[35] J. M. L. Poyato, J. J. Camacho, A. M. Polo, and A. Pardo, Spectrochim. Acta A **51**, 1879 (1995).
[36] J. M. L. Poyato, J. J. Camacho, A. M. Polo, and A. Pardo, Spectrochim. Acta A **52**, 409 (1996).
[37] J. J. Camacho, J. M. L. Poyato, A. M. Polo, and A. Pardo, J. Quant. Spectrosc. Radiat. Transf. **56**, 353 (1996).
[38] M. Lapp and L. P. Harris, J. Quant. Spectrosc. Radiat. Transf. **6**, 169 (1966).
[39] K. M. Mackay, *Hydrogen Compounds of the Metallic Elements* (E. and F. N. Spon, London, 1966), p. 24.
[40] G. Norlen, Phys. Scr. **8**, 249 (1973).
[41] M. D'Orazio and B. Schrader, J. Raman Spectrosc. **2**, 585 (1974).
[42] K. Bergmann and W. Demtröder, J. Phys. B **5**, 1386 (1972); **5**, 2098 (1972).
[43] E. W. Kaiser, J. Chem. Phys. **53**, 1686 (1970).
[44] H. Telle and U. Telle, J. Mol. Spectrosc. **85**, 248 (1981).
[45] W. T. Zemke and W. C. Stwalley, Chem. Phys. Lett. **143**, 84 (1988).
[46] *Handbook of Chemistry and Physics*, 63rd ed. (Chemical Rubber, Cleveland, 1982), p. E-276.
[47] R. J. LeRoy, *Molecular Spectroscopy*, edited by R. F. Barrow, D. A. Long, and D. J. Millin (Chemical Society, London, 1973), Vol. 1, p. 113.
[48] S. C. Yang and W. C. Stwalley, ACS Symp. Ser. **179**, 241 (1982).
[49] G. Herzberg, *Spectra of Diatomic Molecules* (Van Nostrand, New York, 1950).
[50] J. Tellinghuisen, *Photodissociation and Photoionization*, edited by K. P. Lawley (Wiley, New York, 1985), p. 299.
[51] R. B. Kurzel, J. I. Steinfeld, D. A. Hatzenbuhler, and G. E. Leroi, J. Chem. Phys. **55**, 4822 (1971).
[52] S. Lemont and G. W. Flynn, Annu. Rev. Phys. Chem. **28**, 261 (1977).
[53] L. K. Lam, T. Fujiimoto, A. C. Gallager, and M. Hessel, J. Chem. Phys. **68**, 3553 (1978).
[54] T. A. Brunner, R. D. Driver, N. Smith, and D. E. Pritchard, J. Chem. Phys. **70**, 4155 (1979); T. A. Brunner, N. Smith, A. W. Karp, and D. E. Pritchard, *ibid.* **74**, 3324 (1981).
[55] G. Ennen and Ch. Ottinger, J. Chem. Phys. **40**, 127 (1979); **41**, 415 (1979).
[56] W. Demtröder, *Laser Spectroscopy* (Springer, New York, 1981).
[57] T. L. D. Collins, A. J. MacCaffery, J. P. Richardson, and M. J. Wynn, Phys. Rev. Lett. **70**, 3392 (1993).